

Washington University School of Medicine

Digital Commons@Becker

Open Access Publications

2020

IL-17-producing $\gamma\delta$ T cells protect against *Clostridium difficile* infection

Yee-Shiuan Chen

Iuan-Bor Chen

Giang Pham

Tzu-Yu Shao

Hansraj Bangar

See next page for additional authors

Follow this and additional works at: https://digitalcommons.wustl.edu/open_access_pubs

Authors

Yee-Shiuan Chen, Iuan-Bor Chen, Giang Pham, Tzu-Yu Shao, Hansraj Bangar, Sing Sing Way, and David B Haslam

IL-17–producing $\gamma\delta$ T cells protect against *Clostridium difficile* infection

Yee-Shiuan Chen, ... , Sing Sing Way, David B. Haslam

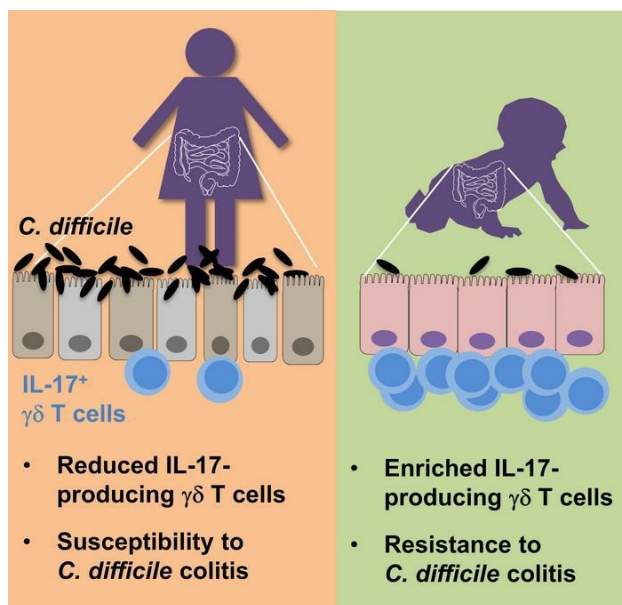
J Clin Invest. 2020;130(5):2377-2390. <https://doi.org/10.1172/JCI127242>.

Research Article

Immunology

Infectious disease

Graphical abstract



Find the latest version:

<https://jci.me/127242/pdf>



IL-17-producing $\gamma\delta$ T cells protect against *Clostridium difficile* infection

Yee-Shiuan Chen,¹ Iuan-Bor Chen,¹ Giang Pham,² Tzu-Yu Shao,² Hansraj Bangar,² Sing Sing Way,² and David B. Haslam²

¹Department of Medicine, Washington University School of Medicine, St. Louis, Missouri, USA. ²Division of Infectious Disease, Cincinnati Children's Hospital Medical Center, Cincinnati, Ohio, USA.

Colitis caused by *Clostridium difficile* infection is a growing cause of human morbidity and mortality, especially after antibiotic use in health care settings. The natural immunity of newborn infants and protective host immune mediators against *C. difficile* infection are not fully understood, with data suggesting that inflammation can be either protective or pathogenic. Here, we show an essential role for IL-17A produced by $\gamma\delta$ T cells in host defense against *C. difficile* infection. Fecal extracts from children with *C. difficile* infection showed increased IL-17A and T cell receptor γ chain expression, and IL-17 production by intestinal $\gamma\delta$ T cells was efficiently induced after infection in mice. *C. difficile*-induced tissue inflammation and mortality were markedly increased in mice deficient in IL-17A or $\gamma\delta$ T cells. Neonatal mice, with naturally expanded ROR γ T⁺ $\gamma\delta$ T cells poised for IL-17 production were resistant to *C. difficile* infection, whereas elimination of $\gamma\delta$ T cells or IL-17A each efficiently overturned neonatal resistance against infection. These results reveal an expanded role for IL-17-producing $\gamma\delta$ T cells in neonatal host defense against infection and provide a mechanistic explanation for the clinically observed resistance of infants to *C. difficile* colitis.

Introduction

Clostridioides difficile (formerly *Clostridium difficile*) is a Gram-positive, spore-forming, anaerobic bacillus that colonizes the large intestine and causes colitis when normal microbiota communities are disrupted. *C. difficile* infection is a major health care-associated infection and is now recognized as the primary cause of infectious diarrhea after hospitalization and treatment with antibiotics (1). In the United States, *C. difficile* was responsible for almost half a million infections and associated with approximately 29,000 deaths in 2011 (2). There is also a rising incidence and severity of *C. difficile* infection (3–7), and community-acquired infection is increasingly recognized (8–10). Clinical symptoms of *C. difficile* infection range from mild diarrhea to severe, life-threatening pseudomembranous colitis, toxic megacolon, and death (11, 12). However, individuals, particularly very young infants, colonized with *C. difficile* are frequently asymptomatic (13, 14).

Intestinal inflammation associated with *C. difficile* infection is primarily mediated by the major virulence factors of toxigenic *C. difficile*, toxins A and B (TcdA and TcdB), on the intestinal epithelium (15). The immune components that protect against *C. difficile* infection are not fully understood, with data suggesting that inflammation can play both protective and pathogenic roles. Several studies have shown that mice with altered innate immune responses, including defects in innate lymphoid cells, IL-1 β expression, and MyD88 signaling, have increased mortality after *C. difficile* infection (16–20). On the other hand, IL-23-deficient mice have decreased inflammation and disease severity (21). We

previously showed that persistent diarrhea in *C. difficile* infection correlates with intestinal inflammation and not fecal pathogen burden in adults and children with *C. difficile* infection (22, 23), which suggests that inflammation may also be responsible for clinically symptomatic infection. Thus, *C. difficile* infection likely involves a complex interplay between the organism, the intestinal microbiome, and local immunological mediators, with disease resolution requiring a balanced inflammatory response that eradicates infection without causing collateral tissue damage (24–27).

Several known features of *C. difficile* epidemiology and pathogenesis led us to examine the role and source of IL-17A in the defense against this pathogen. First, an influx of neutrophils into the mucosa is a characteristic feature of *C. difficile* infection (28), and IL-17 signaling is important for neutrophil recruitment to local tissues during other bacterial infections (29–34). Furthermore, very young infants are highly protected against *C. difficile* infection (13, 14), which is in striking contrast to most other infectious diseases. Whereas immune components protective against microbial infection are typically hyporesponsive in neonates (reviewed in ref. 35), IL-17A-producing $\gamma\delta$ T cells remain relatively abundant and may be particularly important mediators of mucosal defense during the initial stages of postnatal life (36–41). We hypothesize that the temporal and anatomic distribution of IL-17-producing $\gamma\delta$ T cells might contribute to *C. difficile* infection resistance in very young infants. Furthermore, the abundance of IL-17A-producing $\gamma\delta$ T cells is diminished by antibiotic treatment (42), the major risk factor for *C. difficile* infection. Each of these correlative observations led us to investigate whether IL-17 and $\gamma\delta$ T cell are induced by *C. difficile* infection in children and to conduct a more definitive analysis on their potential role in protection.

Here, we report that IL-17 arising from $\gamma\delta$ T cells is a major component of the response to *C. difficile* infection. We found that complementary transcripts encoding IL-17A and the T cell recep-

Conflict of interest: The authors have declared that no conflict of interest exists.

Copyright: © 2020, American Society for Clinical Investigation.

Submitted: January 7, 2019; **Accepted:** January 17, 2020; **Published:** April 6, 2020.

Reference information: *J Clin Invest.* 2020;130(5):2377–2390.

<https://doi.org/10.1172/JCI127242>.

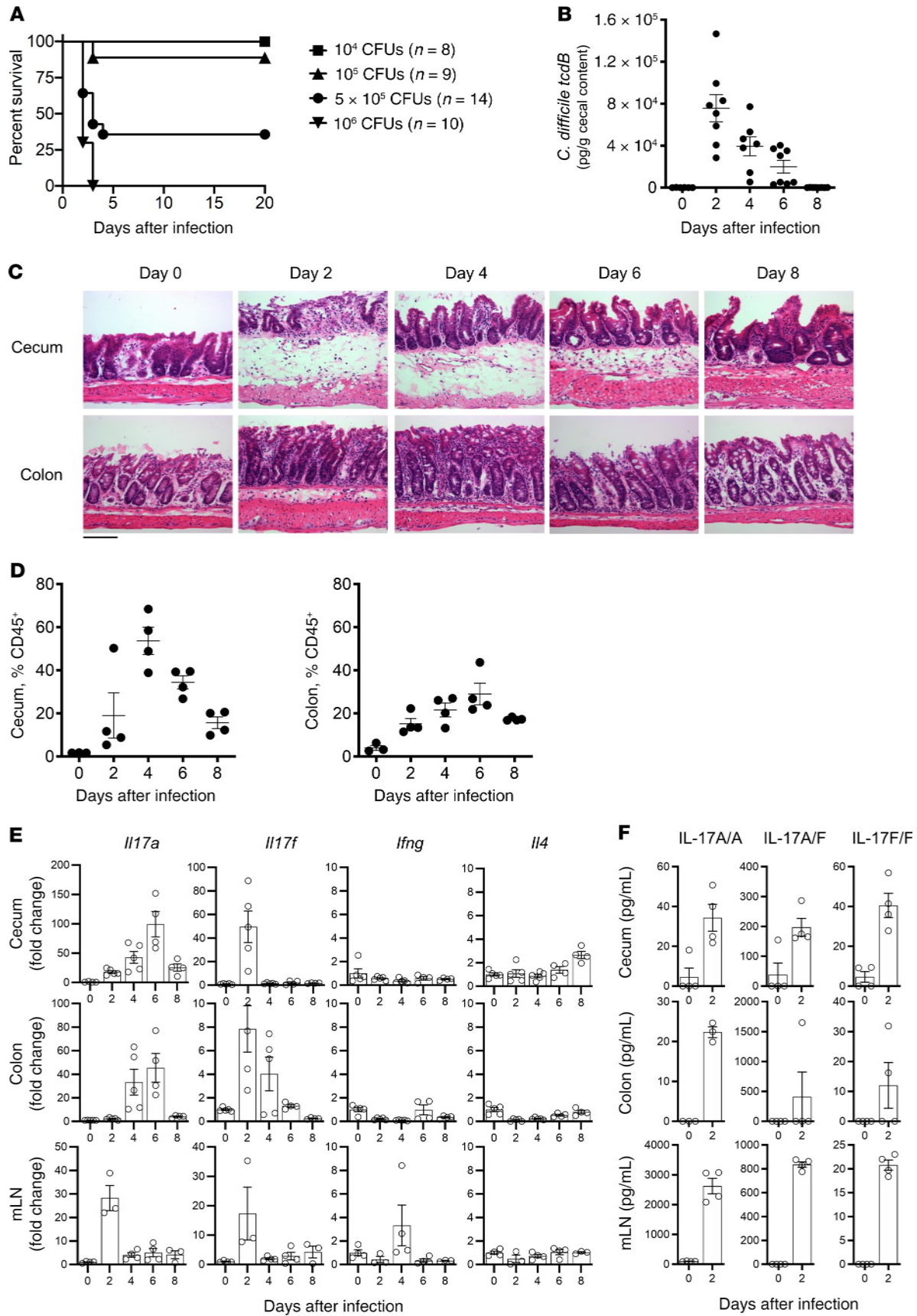


Figure 1. IL-17A expression is increased in the intestines of mice with *C. difficile*. (A) Survival (percentage) of adult WT C57BL/6 mice infected with various CFU of *C. difficile*. (B) *C. difficile* burden was monitored by qPCR analysis of the *tcdB* gene in total cecal content (5×10^5 CFU). $n = 6-8$ per time point. qPCR results were normalized to a standard curve to calculate pg *tcdB* in the input sample. (C) Longitudinal sections of H&E-stained cecum and colon (5×10^5 CFU). Original magnification, $\times 20$; scale bar: 50 μm . (D) Infiltrating leukocytes were analyzed by flow cytometry following *C. difficile* infection (5×10^5 CFU). Gating was done on live CD45⁺ cells. $n = 4$ per time point. (E) Total tissues from cecum, colon, and mLNs of *C. difficile*-infected mice (5×10^5 CFU) were harvested, analyzed by qPCR, and normalized to day-0 samples, with GAPDH used as an endogenous control. $n = 3-5$ per time point. (F) Total cecal and colonic tissues were harvested from *C. difficile*-infected mice (5×10^5 CFU), dissociated, cultured for 24 hours, and the culture supernatant collected and analyzed by ELISA. Single-cell suspensions of mLNs from *C. difficile*-infected mice (5×10^5 CFU) were stimulated with plate-bound anti-CD3 ϵ antibody for 72 hours and similarly analyzed by ELISA. $n = 4$ per time point.

tor (TCR) δ chain were elevated in fecal extracts from infected children, highlighting the idea that these immune components are induced during *C. difficile* infection. We also demonstrate that IL-17-producing $\gamma\delta$ T cells were naturally expanded in neonatal mice and essential for enhanced protection against *C. difficile* infection in this developmental window. Together, these results reveal an essential role for IL-17 produced by $\gamma\delta$ T cells in the defense against *C. difficile* infection.

Results

IL-17 is efficiently induced during C. difficile infection. Various murine models of *C. difficile* infection have been described, with variations in inoculation dosage and antibiotic pretreatment regimes required to achieve consistent infection that likely reflect differences in commensal microbiota composition for mice in each institution (43–48). Experiments were performed at 2 institutions (Washington University in St. Louis, Missouri, USA, and Cincinnati Children's Hospital, Cincinnati, Ohio, USA), where similar susceptibility to *C. difficile* was established after optimizing antibiotic treatment and the infectious dose. At both facilities, age- and sex-matched mice on a C57BL/6 background were exposed to a defined cocktail of antibiotics before oral gavage with *C. difficile* spores and then monitored for weight loss and mortality. In adult mice, we found that doses ranging from 1×10^4 to 1×10^6 CFU caused symptoms of *C. difficile* disease, including ruffled fur, hunched posture, and weight loss, with dose-dependent mortality (Figure 1A). *C. difficile* intestinal burden was monitored by quantitative PCR (qPCR) analysis of the *tcdB* gene, as this approach is more sensitive than culturing (49) and detects endogenous strains of *C. difficile* found in some mouse strains (50, 51). We found that *C. difficile* was absent in antibiotic-treated mice before infection, peaked on day 2, and then declined to nearly undetectable levels by day 8 after infection (Figure 1B). This tempo was further confirmed by histopathological analysis, which revealed the most severe epithelial damage and edema in the cecum 2 days after infection, followed by almost complete recovery by day 8 (Figure 1C). Likewise, leukocyte infiltration into the cecum and colonic lamina propria and expression of proinflammatory and antimicrobial genes peaked on days 2–4 after infection and progressively declined during the recovery phase (Figure 1D and Supplemental

Figure 1; supplemental material available online with this article; <https://doi.org/10.1172/JCI127242DS1>).

Interestingly, intestinal inflammation after *C. difficile* infection was associated with a selective increase in the production of IL-17. Leukocytes recovered from the cecum of infected mice showed a greater than 20-fold increase in the percentage of IL-17A-producing cells but minimal changes in IFN- γ or IL-4 production (Supplemental Figure 2). This paralleled selectively increased expression of *Il17a* and *Il17f* in intestinal tissues and the draining mesenteric lymph nodes (mLNs) (Figure 1E). IL-17A expression was increased by 20-fold and 25-fold in the cecum and mLNs, respectively, by day 2 after infection, whereas only marginal or nonsignificant shifts were found for *Ifng* and *Il4*. IL-17F is frequently coproduced with IL-17A (52, 53), and *Il17f* expression was simultaneously upregulated upon *C. difficile* infection (Figure 1E). In turn, we observed a sharp increase in expression levels of all 3 dimeric forms of IL-17A and IL-17F protein in cecum, colon, and mLNs, beginning 2 days after *C. difficile* infection (Figure 1F). Thus, a robust induction of IL-17 was already well underway at time points when death occurred in mice treated with the highest dose of *C. difficile* inoculum.

IL-17A is essential for host protection against C. difficile infection. To determine the contribution of IL-17A to host protection against *C. difficile* infection, we evaluated potential differences in the susceptibility of IL-17A-deficient mice. We found sharply increased rates of mortality after infection of IL-17-deficient mice compared with isogenic C57BL/6 control mice (Figure 2A). Increased susceptibility paralleled more profound tissue damage, particularly edema and ulceration in the cecum after *C. difficile* infection in IL-17-deficient mice compared with control mice (Figure 2B). We also observed a marked increase in *C. difficile* recovery in the intestinal contents (Figure 2C), along with increased intestinal permeability measured by systemic recovery of orally administered FITC dextran after *C. difficile* infection in IL-17A-deficient mice compared with WT control mice (Figure 2D). There was significantly higher neutrophil infiltration in the colon of IL-17A-deficient mice, probably reflecting the greater severity of disease in these animals (Supplemental Figure 3A). Interestingly however, depletion of granulocytes using the anti-Ly6G antibody did not affect susceptibility, suggesting that neither the presence of neutrophils nor their recruitment through IL-17A-dependent pathways was needed for protection in our model of *C. difficile* infection (Supplemental Figure 3B).

Importantly, these differences in susceptibility could not be explained by potential differences in the intestinal microbiome of these unique mouse strains, since the bedding between cages of these mice was regularly mixed before and after *C. difficile* inoculation. Likewise, we observed increased susceptibility among genetically identical cohoused mice after IL-17A functional neutralization using antibodies (Figure 2E). Taken together, these findings indicate an essential role for IL-17A in protection against epithelial and tissue injury during *C. difficile* infection.

$\gamma\delta$ T cells are the major source of IL-17A following C. difficile infection. Given the critical role of IL-17A in our model of *C. difficile* infection, we sought to determine the cellular source of this cytokine. IL-17A can be produced by multiple cell types, including conventional CD4⁺ Th17 $\alpha\beta$ T cells, CD8⁺ T cells, $\gamma\delta$ T cells,

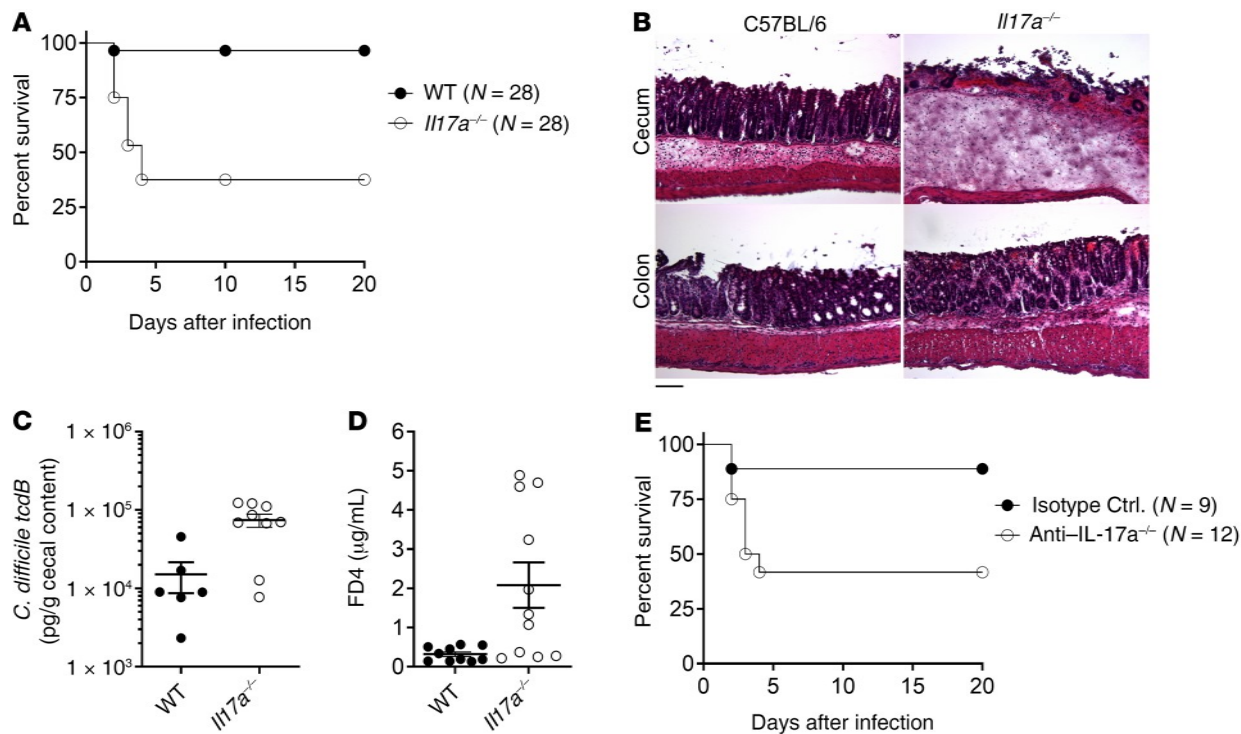


Figure 2. IL-17A is essential for host protection during *C. difficile*. (A) Survival (percentage) of WT and *Il17a*^{-/-} mice following *C. difficile* infection (4×10^5 CFU). $P < 0.0001$, by log-rank test. Data were combined from 3 experiments. (B) Longitudinal sections of H&E-stained sections of cecum and colon from WT and *Il17a*^{-/-} mice on day 2 after infection (4×10^5 CFU). Original magnification, $\times 10$; scale bar: 50 μm . Images are representative of 3 experiments. (C) *C. difficile* burden in WT and *Il17a*^{-/-} mice was monitored by qPCR analysis of the *tcdB* gene in total cecal content on day 2 after infection (4×10^5 CFU). qPCR results were normalized to a standard curve to calculate pg *tcdB* in the input sample. $n = 6$ for WT; $n = 9$ for *Il17a*^{-/-}. (D) WT and *Il17a*^{-/-} mice on day 2 after infection (4×10^5 CFU) were orally gavaged with 4 kDa FD4. Blood was collected via retro-orbital bleeding 3 hours later, and serum fluorescence was measured. Data were combined from 2 experiments. $n = 10$ for WT; $n = 11$ for *Il17a*^{-/-}. (E) Survival (percentage) of WT littermate mice treated with isotype control (MOPC-21) or anti-IL-17A (17F3) antibody after *C. difficile* infection (4×10^5 CFU). $P < 0.05$, by log-rank test. Mice were treated with 1 mg antibody on day -1, followed by 0.5 mg every 48 hours thereafter.

innate lymphoid cells, NK cells, and epithelial cells. We found that both $\alpha\beta$ and $\gamma\delta$ T cells infiltrated the lamina propria in response to *C. difficile* infection in these mice, with a progressive increase in accumulation of each cell T cell subset in the first week after infection (Figure 3A). Interestingly, expression of the activation marker CD69 was substantially higher in intestinal $\gamma\delta$ T cells compared with levels in $\alpha\beta$ T cells after *C. difficile* infection (Figure 3B), whereas only background expression levels were detected for each cell type before *C. difficile* infection (Supplemental Figure 4). Furthermore, $\gamma\delta$ T cells in the mLNs showed increased proliferation upon infection, whereas $\alpha\beta$ T cells remained at baseline levels, as revealed by Ki67 expression (Figure 3C).

Flow cytometric analysis and intracellular staining further showed that $\gamma\delta$ T cells constituted the dominant source of this cytokine in the cecum, colon, and mLNs, accounting for approximately 80% of all IL-17A-producing cells, whereas $\alpha\beta$ T cells constituted less than 10% of these cells in each tissue on day 2 after infection (Figure 4A). An expansion of this analysis revealed that IL-17A production was nearly exclusive to intestinal $\gamma\delta$ T cells within the first week after infection (Figure 4B). We detected a sharp increase in IL-17A production for mLN $\gamma\delta$ T cells by day 2 after infection, whereas cells in the cecum and colon showed delayed kinetics that did not reach peak levels until day 6 after infection (Figure 4B). By contrast, only a small fraction of $\alpha\beta$ T cells produced IL-17A within

the first 6 days after *C. difficile* infection (Figure 4B). Consistent with the role of $\gamma\delta$ T cells in the immediate response to *C. difficile*, *Il17a* transcript levels were unchanged (cecum, colon) or substantially reduced (mLNs) after infection in TCR δ -KO mice (*Tcrd*^{-/-}), which lack all mature $\gamma\delta$ T cells (ref. 54 and Figure 4C). In turn, *Tcrd*^{-/-} mice compared with WT control mice showed increased susceptibility following *C. difficile* infection (Figure 4D). Taken together, these data implicate $\gamma\delta$ T cells as the primary source of protective IL-17A during *C. difficile* infection.

To determine whether IL-17A-producing $\gamma\delta$ cells represent a similar component of the clinical response to *C. difficile* infection, we performed qPCR to quantitate the relative abundance of *IL17A* and TCR δ variables 1 and 3 (*TRDV1/3*) transcripts encoding IL-17A and the TCR δ chain in fecal extracts from children with *C. difficile* infection compared with uninfected controls. Whereas *IL17A* mRNA was detected in only 2 of 16 control samples, 8 of 15 children with *C. difficile* infection had elevated *IL17A* expression. Similarly, this analysis showed detectable *TRDV* expression in the fecal extracts of all (15 of 15) children with *C. difficile* infection, but only in 3 of the 16 control children (Figure 5). Thus, IL-17 and $\gamma\delta$ T cells were both induced by *C. difficile* clinical infection in humans and mice.

C. difficile infection induces activation of $\gamma\delta$ T cells. The importance of IL-17-producing $\gamma\delta$ cells in mucosal barrier protection is increasingly recognized (52, 55–57). However, the signals

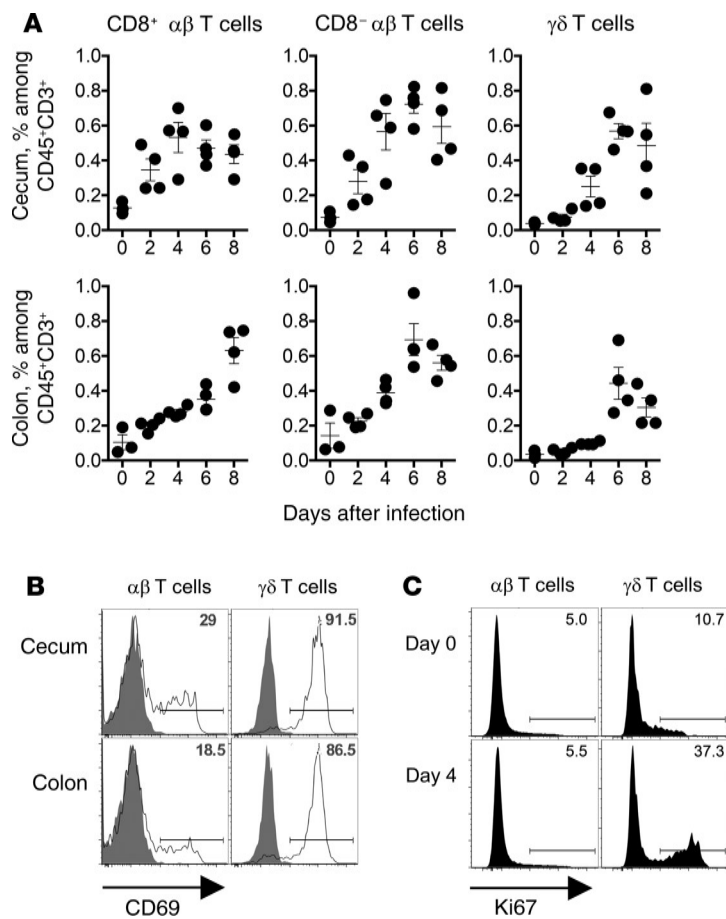


Figure 3. $\gamma\delta$ T cells respond rapidly to *C. difficile*. (A) $\alpha\beta$ T cell and $\gamma\delta$ T cell infiltration into the cecum and colon following *C. difficile* was analyzed by flow cytometry. Gating was done on live CD45⁺CD3⁺ CD8 α^{\pm} TCR β^{\pm} cells or live CD45⁺CD3 ϵ^{\pm} TCR $\gamma\delta^{\pm}$ cells. $n = 4$ per time point. (B) Surface expression of CD69 in $\alpha\beta$ T cells and $\gamma\delta$ T cells on day 4 after infection (4×10^5 CFU). Gray-colored histograms represent isotype control staining. Gating was done on live CD45⁺CD3 ϵ^{\pm} CD4⁺ TCR β^{\pm} cells or live CD45⁺CD3 ϵ^{\pm} TCR $\gamma\delta^{\pm}$ cells (results are representative of 2 experiments). (C) Ki67 expression in $\alpha\beta$ T cells and $\gamma\delta$ T cells from mLN from naive and day-4-infected mice (4×10^5 CFU). Results are representative of 2 experiments. Gating was done as in B.

cells in the intestines of *C. difficile*-infected mice (Supplemental Figure 5). To bypass this limitation, we performed RNA-Seq to evaluate TCR gene usage among sort-purified IL-17A⁺ and IL-17A⁻ $\gamma\delta$ T cells from mice after *C. difficile* infection (Supplemental Figure 6). This analysis showed a limited distribution of TCR usage among $\gamma\delta$ T cells recovered from mLN. Comparison of TCR gene usage between IL-17A⁺ and IL-17A⁻ $\gamma\delta$ T cells revealed that nearly all cytokine-producing cells expressed the genes encoding Trgv6 (58%) or Trgv2 (26%) in association with Trdv4 (98%; Trdv4 was known as V δ 1 in prior nomenclature; ref. 68) (Figure 6B). Thus, IL-17-producing $\gamma\delta$ T cells responsive to *C. difficile* infection showed a highly constrained oligoclonal repertoire dominated by Trgv6 and Trdv4 TCRs and Trgv2 and Trdv4 TCRs. These findings are similar to the recently described clonal expansion of V γ 6⁺V δ 4⁺ cells that provide immunity against *Staphylococcus aureus* infection (69).

To investigate the relative contribution of TCR stimulation for IL-17 production by $\gamma\delta$ T cells, we evaluated cytokine production after stimulation with defined anti-TCR antibodies. This analysis showed more than 100-fold and more than 30-fold increased production of IL-17A/A and IL-17A/F, respectively, by $\gamma\delta$ T cells recovered from the mLN of *C. difficile*-infected mice in response to anti-CD3 or anti-TCR $\gamma\delta$ stimulation (Figure 6C). In turn, several studies have reported that IL-1 β and IL-23 can also independently drive IL-17A production by $\gamma\delta$ T cells (29, 70–72). We obtained similar results, since comparable production of IL-17 was achieved after stimulation with IL-1 β and IL-23 versus stimulation with anti-TCR antibodies (Figure 6C). Interestingly, however, IL-17 production increased dramatically with combined IL-1 β /IL-23 and anti-TCR stimulation, highlighting the synergistic effects of these proinflammatory cytokines and cognate antigen TCR stimulation in promoting the activation of $\gamma\delta$ T cells. These results are consistent with increased IL-1 β and IL-23 responsiveness after $\gamma\delta$ TCR stimulation, which in turn results in amplified IL-17 production (60).

$\gamma\delta$ T cells are produced in waves during embryonic development, with TCR chain expression closely tracking the stage of development. Those cells expressing Trgv6 are produced in the thymus exclusively during embryogenesis, whereas cells bearing Trgv2 develop later in gestation or in the early newborn period (58, 61). The IL-17 effector fate of Trgv6-producing cells is determined before thymic egress, whereas development of the IL-17 effector fate for other TCR-expressing $\gamma\delta$ subsets is less well described. Several recent studies demonstrated characteristic features of $\gamma\delta$ cells that acquire an IL-17 effector fate during embryogenesis (57, 68, 73–76). Cell-surface labeling showed these $\gamma\delta$ cells to be nega-

mediating their activation and the unique molecular features of these cells have not been fully described, particularly during the response to infection. Previous studies have shown that $\gamma\delta$ T cells are activated in part through nonclonal receptors, such as NK cell receptors and TLRs (58, 59). However, we found that expression of NK receptors (NK1.1, NKG2A, NKG2D, NKP46) by $\gamma\delta$ T cells in the intestines of *C. difficile*-infected mice was sharply reduced compared with expression of the IL-17-promoting transcriptional regulator ROR γ (Figure 6A). Other potential activation signals for $\gamma\delta$ T cells include stimulation through each cell's respective TCR (60). However, despite their potential for responding to a broad array of antigens through somatic rearrangement of V (variable), D (diversity), and J (joining) gene segments, oligoclonal subsets sharing the same TCR γ and TCR δ chains in specific tissues are often described, probably having populated distinct sites during embryonal and postnatal development (61, 62). For example, $\gamma\delta$ T cells in the dermal layers primarily express TCR γ variable 5 (Trgv5) (International ImMunoGeneTics [IMGT] [http://www.imgt.org], nomenclature is used throughout refs. 63–65), whereas $\gamma\delta$ intraepithelial cells (IELs) primarily express Trgv7 (64, 66). IL-17-producing $\gamma\delta$ cells predominantly bear Trgv6 (61, 67), although under certain circumstances, IL-17-producing $\gamma\delta$ cells may produce Trgv4 or, rarely, Trgv2 or Trgv3 instead of Trgv6.

We examined TCR receptor expression using commercially available antibodies recognizing Trgv1, Trgv4, Trgv5, and Trgv7 and found that they did not label a majority of the IL-17-producing $\gamma\delta$ T

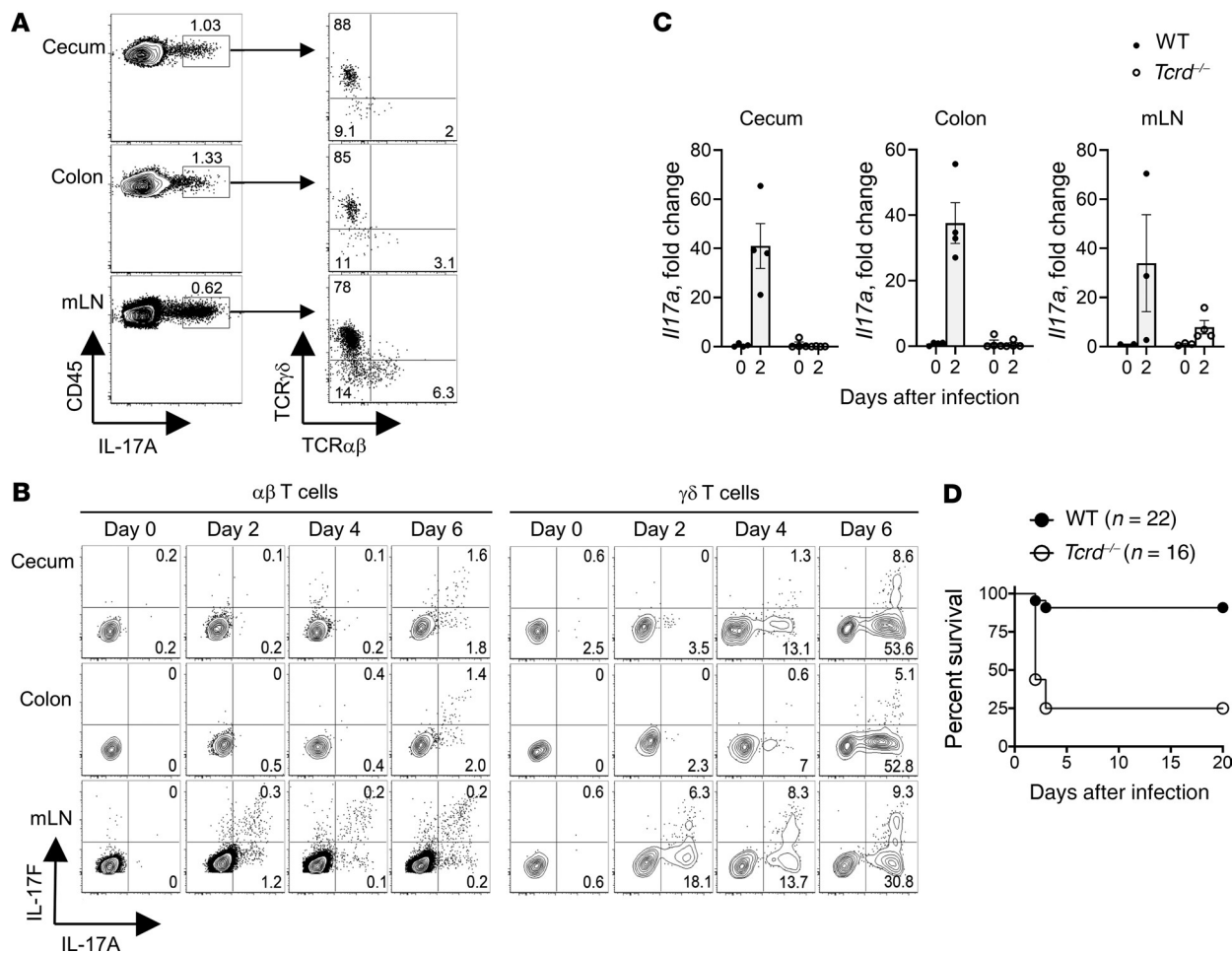


Figure 4. $\gamma\delta$ T cells are the major source of IL-17A and essential for host defense. (A) Single-cell suspensions from tissues from day-4-infected mice (4×10^5 CFU) were stimulated with PMA and ionomycin in vitro, followed by intracellular staining and flow cytometric analysis. Gating was done on live CD45⁺ cells (results are representative of 2 experiments). (B) Single-cell suspensions from tissues of infected mice (4×10^5 CFU) were stimulated with PMA and ionomycin in vitro followed by intracellular staining and then analyzed by flow cytometry. Gating was done on live CD45⁺CD3 ϵ ⁺CD8 α ⁻ TCR β ⁺ cells or live CD45⁺CD3 ϵ ⁻ TCR $\gamma\delta$ ⁺ cells. (C) Total tissues from cecum, colon, and mLNs from naive and day-2-infected mice (4×10^5 CFU) were harvested and analyzed by qPCR for gene expression (solid circles represent WT mice; open circles represent *Tcrd*^{-/-} mice). Results were normalized to day-0 samples, with GAPDH used as an endogenous control. $n = 4$ per time points per genotype. (D) Survival (percentage) of WT and *Tcrd*^{-/-} mice following *C. difficile* infection (4×10^5 CFU). $P < 0.0001$, by log-rank test. Data were combined from 2 experiments.

tive for TNF receptor family member CD27 (77) and positive for the IL-7 receptor CD127 (78), as expected for IL-17-producing $\gamma\delta$ cells (Figure 6D). We further analyzed the aforementioned RNA-Seq data and, as expected, found that IL-17-producing $\gamma\delta$ T cells isolated from *C. difficile*-infected animals expressed high levels of *Rorc*, *Blk*, *Sox13*, and *Zbtb16* transcription factors, *Il17a* and *Il17f* cytokines, and the cytokine receptors *Il1r1* and *Il23r* (Figure 6E), all of which have been described to promote developing IL-17-producing $\gamma\delta$ T cells and effector function (65,79–81). Conversely, *Tcf7*, a negative regulator that is downregulated during T $\gamma\delta$ 17 cell development (64, 65), was markedly repressed (Figure 6E). As expected, expression of *Stat3*, *Irf4*, and *Batf*, transcription factors essential for promoting Th17 differentiation in conventional CD4⁺ $\alpha\beta$ cells, was also reduced, whereas expression of the Th17 repressor *Maf*, which is essential for IL-17-producing $\gamma\delta$ cell development (82), was upregulated in IL-17A⁺ $\gamma\delta$ T cells (Figure 6E). Thus, $\gamma\delta$ cells responding to *C. difficile* infection are characteristic of those previously demonstrated to acquiring effector fate in utero.

Neonatal resistance to *C. difficile* infection is dependent on IL-17 and $\gamma\delta$ cells. Newborn infants are naturally resistant to *C. difficile* infection (13, 14). To investigate whether natural immunity against *C. difficile* during the neonatal period occurs similarly in mice, we evaluated the susceptibility of 7-day-old neonatal mice compared with 6- to 8-week-old adult mice. Remarkably, we found at least a 100-fold increase in resistance to *C. difficile* infection among neonatal mice compared with adult mice. The adult mice showed progressively increased susceptibility after infection with 10^4 , 10^5 , and 10^6 CFU, whereas death did not occur for neonatal mice infected with these same *C. difficile* inocula (Figure 7A).

Given the critical role for IL-17A during *C. difficile*, as well as the identification of $\gamma\delta$ T cells as the source of IL-17A, we hypothesized that newborn infants have a greater capacity to expand this cell population upon encountering *C. difficile*, which may account for the known resistance of very young infants to *C. difficile* infection. To explore this further, we examined the relative abundance of $\gamma\delta$ T cells compared with $\alpha\beta$ T cells in the intestinal tissues of

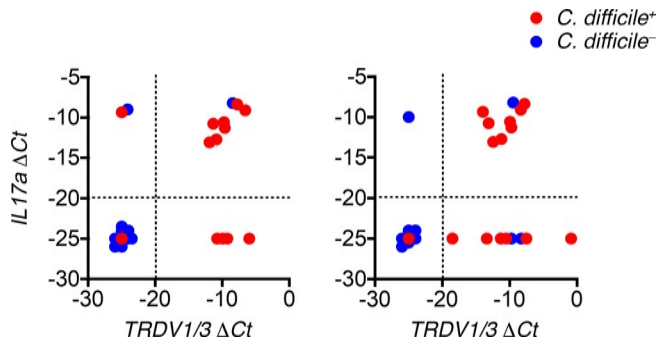


Figure 5. IL-17 and TCR γ chain transcripts are detected in fecal extracts from children with *C. difficile* infection. Total nucleic acids in stool samples from *C. difficile* culture–positive patients and control patients were analyzed by qPCR. Results were normalized to GAPDH (red circles indicate *C. difficile*⁺ patients, *n* = 15; blue circles indicate control patients, *n* = 15).

neonatal mice compared with adult mice. We found that $\gamma\delta$ T cells were substantially enriched among the intestinal lamina propria and mLNs of neonatal mice compared with adult mice, with only a marginal difference in the percentage $\alpha\beta$ T cells (Figure 7B). Importantly, a majority of $\gamma\delta$ T cells in neonatal mice were ROR γ t⁺ before infection (Figure 7C), and IL-17 production was sharply increased after *C. difficile* infection among $\gamma\delta$ T cells in neonatal mice versus production in adult mice (Figure 7D).

We used complementary loss-of-function approaches to investigate the necessity of $\gamma\delta$ T cells for enhanced resistance of neonatal mice to *C. difficile* infection. Neonatal *Il17a*^{-/-} and *Tcrd*^{-/-} mice, each compared with age-matched WT control mice, were highly susceptible to infection (Figure 7E). We also observed a sharp increase in susceptibility of neonatal mice after administration of anti-IL-17A or anti-TCR $\gamma\delta$ antibodies, whereas normal resistance was not affected in littermate control neonatal mice treated with anti-TCR $\alpha\beta$ or isotype control antibodies (Figure 7F). In line with the findings of prior studies in adult mice (83), we found that $\gamma\delta$ T cells were not depleted in neonatal mice treated with anti-TCR $\gamma\delta$ antibody (clone UC7-13D5). However, TCRs were functionally neutralized, since staining with an alternative anti-TCR $\gamma\delta$ antibody clone (GL3) was efficiently eliminated, and the increased susceptibility phenotype was identical to that of *Tcrd*^{-/-} neonatal mice (Figure 7, E and F). Importantly, we found that susceptibility did not further increase among neonatal mice simultaneously administered IL-17A and $\gamma\delta$ T cell–neutralizing antibodies (Figure 7G). These nonadditive effects highlight $\gamma\delta$ T cells as an important cellular source of IL-17 that protects neonatal mice against *C. difficile* infection.

Discussion

IL-17 has been implicated in the development of chronic inflammation and autoimmunity. Preclinical infection models show that it is also essential for host defense against bacterial and fungal pathogens and in maintaining homeostasis, particularly at mucosal epithelial surfaces (55, 84). The dual roles of IL-17 appear to be conserved in humans, as heightened levels of expression have been linked to the development of Crohn's disease and psoriasis, whereas patients genetically deficient in *IL17RA* or expressing a

dominant-negative form of *IL17F* are susceptible to mucocutaneous candidiasis. Protective roles for IL-17 in the defense against bacterial infections, including *E. coli*, *B. subtilis*, and *L. monocytogenes*, are also well described (29, 85, 86).

C. difficile infection causes profound damage of the intestinal mucosa in susceptible individuals, suggesting that IL-17 defenses may have an impact on the outcome of this disease. Indeed, we demonstrated that IL-17 was selectively produced in intestinal tissues following *C. difficile* infection. IL-17 message and protein were both sharply induced within 2 days of infection, the point at which infected animals begin to become ill and, at higher infectious doses, succumb to disease. Strikingly, animals with impaired IL-17 responses through gene knockout or antibody neutralization had increased mortality after *C. difficile* infection, directly implicating this cytokine in protection against disease.

IL-17 can arise from several cell types in the intestine, including CD4⁺ $\alpha\beta$ T cells (Th17 cells), innate lymphoid cells (ILC3 cells), and $\gamma\delta$ T cells. We investigated the cellular source of intestinal IL-17 at the critical early time points during *C. difficile* infection and found that $\gamma\delta$ cells accounted for almost the entire IL-17–staining cell population. In turn, *IL17A* and *TRDV* mRNA, encoding IL-17A and the TCR δ chain, respectively, were present in most children with *C. difficile* infection but were rarely detected in uninfected children. Correspondingly, TCR δ chain–deficient animals unable to produce $\gamma\delta$ cells were almost devoid of intestinal *Il17* gene expression following *C. difficile* infection. As expected, given their lack of IL-17 responsiveness, these animals had sharply increased susceptibility to *C. difficile*, with nearly identical mortality kinetics compared with IL-17A–deficient mice.

The principal function of IL-17A has largely been attributed to neutrophil recruitment to inflammatory sites, and recent reports examining the susceptibility of *Nod1*^{-/-} and *Myd88*^{-/-} mice have linked impaired neutrophil recruitment with worse outcomes following *C. difficile* infection (17, 18). In our model, *Il17a*^{-/-} mice showed no defect in neutrophil infiltration into the intestines. Further, we examined the role of neutrophils in the defense against infection in our model and found no impact on survival after neutrophil depletion. Our results are similar to those of McDermott et al., who reported no effect on outcomes of *C. difficile* infection following neutrophil depletion with the anti-GR1 antibody used in our studies. Similarly, GM-CSF treatment decreased neutrophil infiltration into the intestines of *C. difficile*–infected mice but did not affect survival (87). It should be noted that our results are in contrast with those of other studies, including the one by Nakagawa et al., which showed that *Il17a*^{-/-} mice on the BALB/c genetic background were protected from *C. difficile* infection (88). Further, Jarchum et al. found increased mortality in *C. difficile*–infected mice after neutrophil depletion using the antibody 1A8, independent of IL-17 manipulation (17). Although the factors responsible for these discrepant results are unclear, we surmise that differences in mouse strain, experimental protocol, and commensal flora (19) may be contributing factors. The contribution of host immunity to defense against *C. difficile* infection is exceptionally complex, as might be expected for an infection that causes widespread injury to the intestinal mucosa. Components of the innate and adaptive immune systems have been shown to contribute to defense, and yet marked inflammation is a hallmark of

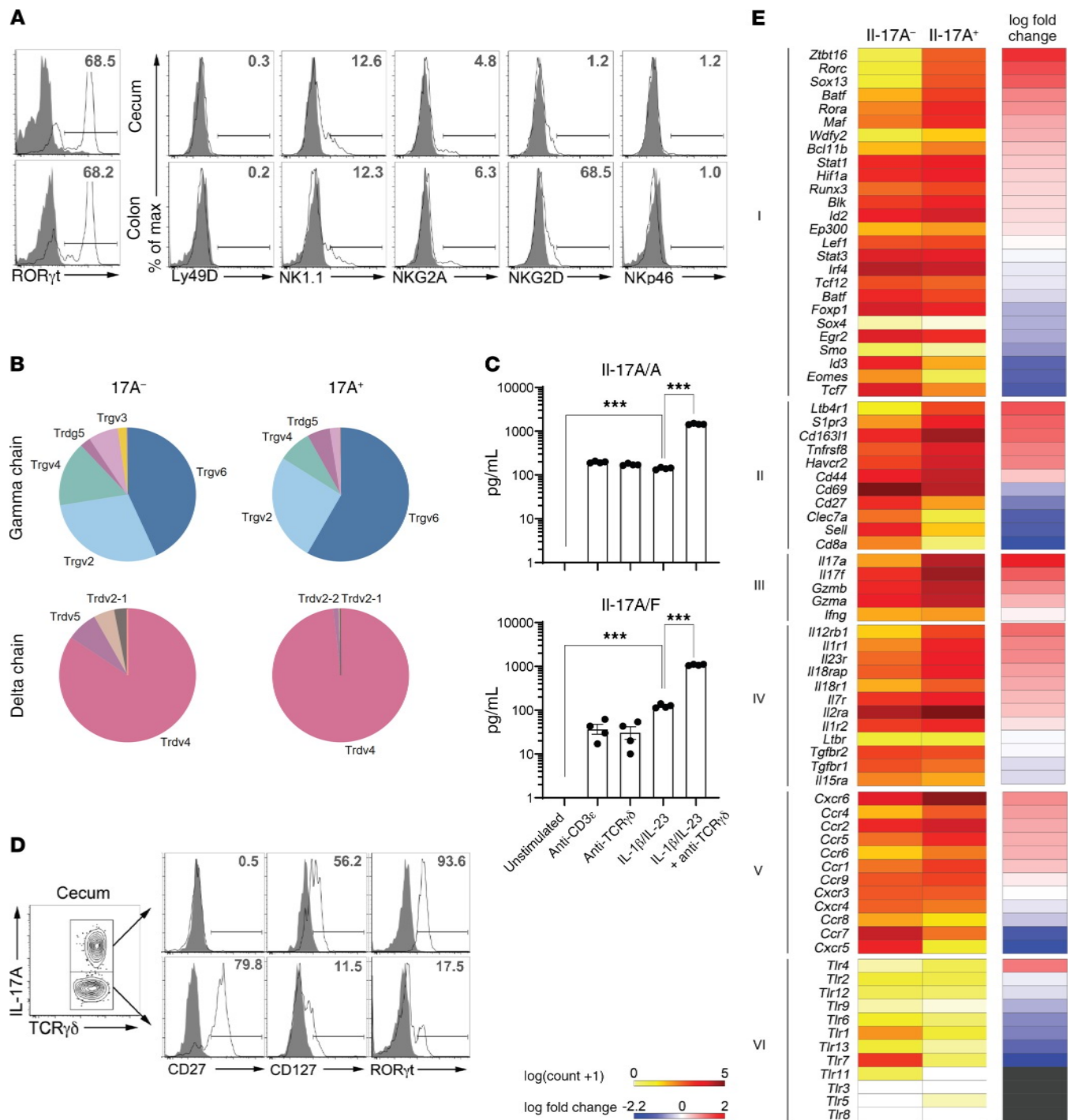


Figure 6. *C. difficile*-responsive IL-17A⁺ $\gamma\delta$ T cells bear a restricted subset of TCR and have a distinctive phenotype. (A) Single-cell suspensions from cecum and colon from day-4-infected mice (4×10^5 CFU) were analyzed by flow cytometry. Gating was done on live CD45⁺CD3 ϵ ⁺ TCR $\gamma\delta$ ⁺ cells. Gray-colored histograms represent the isotype control staining. max, maximum. (B) Distribution of V γ and V δ gene usage of IL-17A⁻ and IL-17A⁺ mLN $\gamma\delta$ T cells from day-4-infected mice (4×10^5 CFU). mLN $\gamma\delta$ T cells were isolated (see also Supplemental Figure 6) and stimulated in vitro with PMA and ionomycin and labeled by surface cytokine capture. Gene expression was analyzed by RNA-Seq. (C) $\gamma\delta$ T cells from mLN from day-4-infected mice (4×10^5 CFU) were isolated by magnetic beads and cultured for 72 hours with the indicated stimuli (anti-CD3 ϵ , anti-TCR $\gamma\delta$, 10 μ g/mL; IL-1 β /IL-23, 10 ng/mL). $n = 4$ per group. Supernatants were then collected analyzed by ELISA. (D) Single-cell suspensions from cecum and colon from day-4-infected mice (4×10^5 CFU) were stimulated with PMA and ionomycin in vitro, followed by intracellular staining and then flow cytometric analysis. Gating was done on live CD45⁺CD3 ϵ ⁺ TCR $\gamma\delta$ ⁺ cells. (E) Heatmap representation of selected genes from RNA-Seq analysis of sorted mLN $\gamma\delta$ T cells from day-4-infected mice (4×10^5 CFU). Cells were stimulated in vitro with PMA and ionomycin and labeled by surface cytokine capture, followed by sorting, as in Supplemental Figure 6. I, transcription factors; II, surface receptors; III, effector molecules; IV, cytokine receptors; V, chemokine receptors; VI, TLRs.

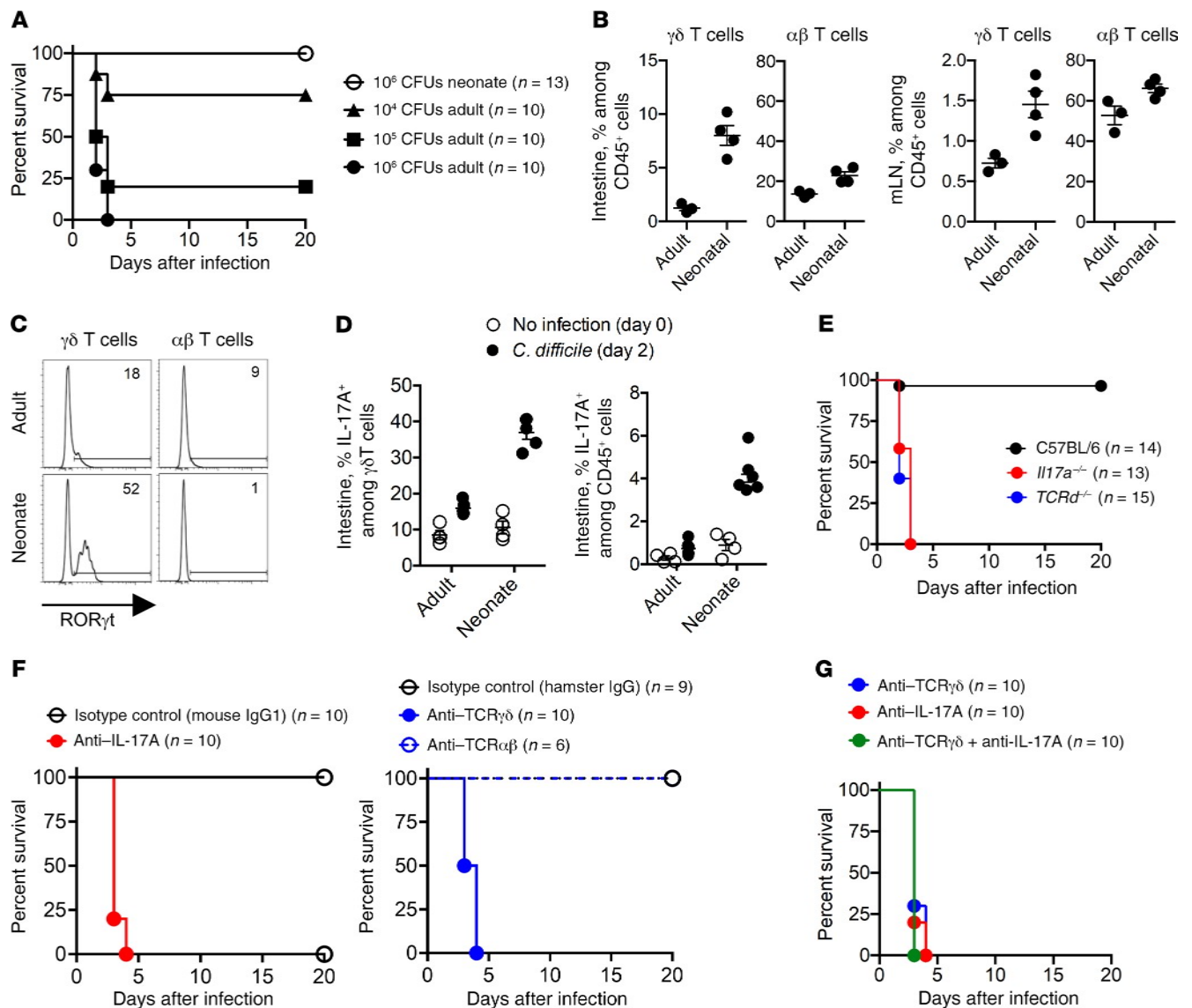


Figure 7. IL-17 and $\gamma\delta$ T cells are more abundant in newborn mice and essential for enhanced protection against *C. difficile* infection compared with adult mice. (A) Survival (percentage) of WT C57BL/6 adult and neonatal mice infected with various CFU of *C. difficile*. (B) $\alpha\beta$ T cells and $\gamma\delta$ T cells from uninfected adult and neonatal mice were analyzed by flow cytometry. Gating was done on live CD45⁺CD3⁺TCR β ⁺ cells or live CD45⁺CD3⁺TCR $\gamma\delta$ ⁺ cells. $n = 4$ per group. (C) ROR γ t expression in $\alpha\beta$ T cells and $\gamma\delta$ T cells from uninfected adult and neonatal mice were analyzed by flow cytometry. Gating was done on live CD45⁺CD3⁺TCR β ⁺ cells or live CD45⁺CD3⁺TCR $\gamma\delta$ ⁺ cells. Results are representative of 2 experiments. (D) Single-cell suspensions from intestines from adult and neonatal day-2-infected mice (1×10^6 CFU) were stimulated with PMA and ionomycin in vitro, followed by intracellular staining and flow cytometric analysis. Gating was done on live CD45⁺CD3⁺TCR $\gamma\delta$ ⁺IL-17A⁺ cells. $n = 4$ –6 per group. (E) Survival (percentage) of neonatal WT, *Il17a*^{-/-}, and *Tcrd*^{-/-} mice following *C. difficile* infection (1×10^6 CFU; WT vs. *Il17a*^{-/-} and WT vs. *Tcrd*^{-/-}; $P < 0.0001$, by log-rank test). (F) Survival (percentage) of WT neonatal littermate mice treated with isotype control (MOPC-21 or Armenian hamster IgG), anti-IL-17A (17F3), anti-TCR $\gamma\delta$ (UC7-13D5), or anti-TCR $\alpha\beta$ (H57-597) after *C. difficile* infection (1×10^6 CFU). $P < 0.05$, by log-rank test. Neonatal mice received 100 μ g antibody on day -2, followed by a second dose on day 0. (G) Survival (percentage) of WT neonatal littermate mice treated with isotype controls (MOPC-21 and Armenian hamster IgG), anti-IL-17A (17F3), or anti-TCR $\gamma\delta$ (UC7-13D5) plus anti-IL-17A following *C. difficile* infection (1×10^6 CFU. Anti-IL-17A vs. anti-TCR $\gamma\delta$ vs. anti-IL-17A plus anti-TCR $\gamma\delta$; $P = 0.20$, by log-rank test). Neonatal mice received 100 μ g antibody on day -2, followed by a second dose on day 0.

the disease and accounts for the clinical features of severe *C. difficile* colitis (22, 23). Murine models of *C. difficile* disease highlight the multifactorial roles of innate responses in the defense against acute infection, while also demonstrating that the same responses may be protective in some experimental conditions but harmful in others. For example, Myd88 and IL-1 β are protective against infection (17, 19), yet specific blockade of inflammasome activa-

tion and IL-1 β was protective against intestinal inflammation and injury (89). Finally, we show that $\gamma\delta$ cells mediated defense via the release of IL-17A, yet prior studies demonstrated that Rag1-deficient mice lacking all $\alpha\beta$ and $\gamma\delta$ T cells were not more susceptible to *C. difficile* infection (16, 90, 91). In those reports, innate lymphoid cells (ILCs) were shown to mediate protection. Rag1-deficient mice have expanded numbers of IL-17- and IL-22-producing

ROR γ t⁺ ILCs that produce excessive amounts of cytokines and antimicrobial peptides (92, 93) and therefore probably masked the contribution of IL-17-producing $\gamma\delta$ cells to the defense against *C. difficile* infection.

The developmental features and physiologic functions of IL-17-producing $\gamma\delta$ cells are coming into focus through much recent research (52, 68, 73–75, 82, 94–96). A point of interest has been the relative contribution of TCR stimulation and cytokine signaling in activation. IL-1 β and IL-23 are known to activate IL-17 production in developmentally programmed $\gamma\delta$ cells, whereas TCR signaling has typically been regarded as inessential (57, 62, 97, 98). We found that cytokine and TCR stimulation alone stimulated the production of comparable levels of IL-17 from *C. difficile*-responsive $\gamma\delta$ cells. However, combined stimulation resulted in markedly increased IL-17 production, a finding consistent with recent studies suggesting that TCR signaling may enhance activation through upregulated expression of cytokine receptors, effectively licensing cells for high-level activation (60, 77, 99). The TCR may also contribute to the recently identified capacity for $\gamma\delta$ cells to develop a memory phenotype and expand in response to reinfection when they often have the capacity to coproduce IL-17A and TNF- α (100, 101).

The contribution of TCR signaling to IL-17 release prompted us to investigate TCR gene usage by these cells. We found that the vast majority expressed the γ chains Trgv6 or Trgv2 in association with the δ chain Trdv4. Trgv6- and Trdv4-expressing cells are known to arise during early embryogenesis and acquire effector function before thymic egress. These cells have a distinctive expression pattern of transcription factors and cytokine receptors enabling eventual IL-17 production (38, 64, 65, 102). In the present study, we demonstrated by flow cytometry and transcriptional analysis that *C. difficile*-responsive IL-17-producing $\gamma\delta$ T cells shared characteristic features of embryo-derived IL-17-producing $\gamma\delta$ T cells (64, 65, 102), including their CD27⁺CD127^{hi}ROR γ t⁺ phenotype and increased expression of *Il1r1*, *Il1r2*, *Il23r*, *Rorc*, *Sox13*, *Zbtb16*, and *Cd163l1*.

IL-17-producing $\gamma\delta$ T cells arise in the embryonic thymus and populate the periphery during a confined stage of in utero development (73–75, 94). During challenge, such as mucosal infection, the response of IL-17-producing $\gamma\delta$ T cells typically occurs through proliferation from a preexisting population of fully programmed progenitor cells. In mice, the size of the IL-17-producing $\gamma\delta$ T cell progenitor pool wanes with age, leading to a decreased capacity for IL-17 secretion from the $\gamma\delta$ pool after the newborn period. Similar findings have been observed in humans (36–39, 41, 103). For example, IL-17-producing $\gamma\delta$ T cells are much more abundant in the peripheral blood of newborns than in adults (103), and $\gamma\delta$ T cells are found at greatest abundance in the intestines of full-term newborn infants (41). It has long been recognized that adults are more prone to severe disease and poor outcomes than are young children infected with *C. difficile*. Remarkably, up to 65% of children are colonized with *C. difficile* within the first year of life but fail to manifest disease, whereas by age 3, the presence of *C. difficile* generally causes intestinal inflammation and injury (104). We hypothesized that the greater abundance of intestinal IL-17-producing $\gamma\delta$ T cells during the first several months of life may account, at least in part, for the age dependent-changes in

C. difficile susceptibility during childhood. To test this hypothesis, we first demonstrated that neonatal mice, like infants, are markedly resistant to *C. difficile* infection. Consistent with the enhanced number of IL-17-producing $\gamma\delta$ cells observed in infants, we found higher levels of these cells in the intestines of neonatal mice compared with adult mice. Complementary loss-of-function approaches using neonatal mice with targeted genetic defects in IL-17A or TCR δ , or functional neutralization of each with antibodies, confirmed the necessity of each in enhanced neonatal resistance to *C. difficile* infection.

Taken together, our findings highlight the importance of IL-17 production by $\gamma\delta$ T cells in host defense against *C. difficile* infection. The naturally expanded pool of these cells in intestinal tissue in neonates explains the unique resistance of infants to *C. difficile* infection. Thus, the abundance of IL-17-producing $\gamma\delta$ T cells dictates *C. difficile* infection susceptibility, and enhancing the accumulation of these cells represents an exciting new therapeutic approach for preventing infection by this emerging human pathogen.

Methods

Stool collection. Stool samples from *C. difficile* culture-positive children were collected at the St. Louis Children's Hospital (SLCH), a tertiary pediatric center in St. Louis, Missouri, between June 2011 and July 2012, and stored at -80°C . The SLCH microbiology laboratory uses a flowchart for the diagnosis of *C. difficile*, starting with a glutamate dehydrogenase (GDH) enzyme immunoassay (EIA) (Wampole C. Diff QUIK CHEK). If this test is positive, it is confirmed with the GeneXpert *C. difficile* PCR system (Cepheid). We excluded children whose residual stools were less than 1 mL in volume. We included inpatient, outpatient, and emergency department visits and had no limitations on patients' age or underlying disease. We also enrolled a convenience sample of symptomatic controls: a study team member, when present, stored available stool samples from children diagnosed with bacterial gastroenteritis or who had diarrheal stools with negative bacterial cultures, within 48 hours of receipt.

Mice. All mice used were 7- to 9-week-old adults unless otherwise specified. C57BL/6 mice were purchased from The Jackson Laboratory. *Il17a*^{-/-} mice were provided by Yoichiro Iwakura (University of Tokyo, Tokyo, Japan). *Tcrd*^{-/-} mice were provided by Anthony French (Washington University in St. Louis, St. Louis, Missouri, USA).

All mice were bred and maintained in the specific pathogen-free animal facility at the Washington University School of Medicine or the specific pathogen-free animal facility at Cincinnati Children's Hospital. At Washington University, the animals were housed in static polysulfone microisolators (Allentown) with 1/8-in. Bed-o'Cobs Corncob bedding (Andersons Lab Breeding). Animals were fed PicoLab Rodent Diet 20 (Purina 5053) and received autoclaved sterile city tap water. At Cincinnati Children's Hospital, the animals were housed in static microisolator cages (Alternative Design Manufacturing and Supply) with 1/4-in. Bed-o'Cobs bedding (Andersons Lab Breeding). The animals were fed a Laboratory Autoclavable Rodent Diet 5010 (LabDiet) and received autoclaved water purified by reverse osmosis. All cage components (bottom, lid, wire hopper, feed), bedding, water bottles, nestlets, and enrichment were sterilized by autoclave. NuAire Class II Type A2 Biological Safety Cabinets were used for cage changes. Health surveillance was performed using 6- to 8-week-old, outbred female sentinels (CD-1 or

SW from Charles River Laboratories or Taconic, respectively) that received dirty bedding from each cage on the rack during weekly or biweekly cage changes. One sentinel cage was placed per side of the ventilated racks, approximately every 70–80 cages. Every 12 weeks, a sentinel was bled for serology to assess antibodies against *Mycoplasma pulmonis*, cilia-associated respiratory (CAR) bacillus, ectromelia virus, epizootic diarrhea of infant mice (EDIM), hantaan, K virus, lymphocytic choriomeningitis mammarenavirus (LCMV), myeloblastosis-associated virus types 1 and 2 (MAV1 and MAV2), murine cytomegalovirus (MCMV), mouse hepatitis virus (MHV), metapneumovirus (MPV), mammary tumor virus (MTV), minute virus of mice (MVM), polyoma, pneumonia virus of mice (PVM), reovirus 3 (REO3), Sendai virus, Theiler's murine encephalomyelitis virus (TMEV), and *Encephalitozoon cuniculi*. Feces and fur swabs were also collected every 12 weeks for PCR evaluation of *Aspiculuris tetraptera*, *Myocoptes musculinus*, *Radfordia/Myobia*, *Syphacia muris*, and *Syphacia obvelata*.

Antibodies. The following antibodies were purchased from BioLegend: Alexa Fluor 700 anti-CD45 (30-F11), APC/Cy7 anti-CD3 ϵ (145-2C11), APC/Cy7 anti-CD8 α (53-6.7), APC/Cy7 anti-CD19 (6D5), APC/Cy7 anti-CD45 (30-F11), FITC anti-CD11b (M1/70), FITC anti-IL-17A (TC11-18H10.1), FITC anti-TCR $\gamma\delta$ (GL3), FITC anti-CD3 ϵ (145-2C11), FITC rat IgG1, κ isotype (RTK2071), PE Armenian hamster IgG isotype (HTK888), PE rat IgG1, κ isotype (RTK2071), PE rat IgG2a, κ isotype (RTK2578), PE rat IgG2b, κ isotype (RTK4530), PE mouse IgG1, κ isotype (MOPC-21), PE anti-NK1.1 (PK136), PE anti-NKG2D (A10), PE anti-NKp46 (29A1.4), PE anti-Ly6G (1A8), PE anti-Ly49D (4E5), PE anti-NKG2A (16A11), PE anti-CD8 α (53-6.7), PE anti-CD69 (H1.2F3), PE anti-IFN- γ (XMG1.2), PE anti-IL-4 (11b11), PE anti-IL-17F (9D3.1C8), PE anti-CD27 (LG.3A10), PE anti-V γ 1 (2.11), PE anti-V γ 4 (UC3-10A6), PE anti-V γ 5 (536), PE/Cy7 anti-CD11b (M1/70), PerCP/Cy5.5 anti-TCR β (H57-597), PerCP/Cy5.5 anti-CD19 (6D5), APC anti-TCR $\gamma\delta$ (GL3), low endotoxin, azide-free-purified (LEAF-purified) anti-CD3 ϵ (143-2C11), and LEAF-purified anti-TCR $\gamma\delta$ (GL3). Anti-CD16/CD32 Fc block (2.4G2) and BV650 anti-ROR γ t (Q31-378) were purchased from BD Biosciences. FITC anti-Ki67 (SolA15) and PE anti-ROR γ t (B2D) were purchased from eBioscience. The following antibodies were purchased from Bio X Cell: rat IgG2a isotype control (2A3), anti-Ly6G (1A8), mouse IgG1 isotype control (MOPC-21), anti-IL-17A (17F3), Armenian hamster IgG isotype control, anti-TCR $\gamma\delta$ (UC7-13D5), and anti-TCR β (H57-597). PE anti-V γ 7 (F2.67) was a gift from Pablo Pereira (Institute Pasteur, Paris, France).

***C. difficile* infection.** *C. difficile* spores were prepared as previously described (94). Briefly, *C. difficile* (VPI10463) spores were streaked on anaerobic blood agar plates and grown anaerobically using the GasPak system for 6 days to induce sporulation. Collected spores were then washed in PBS and heat-shocked at 56°C for 10 minutes to kill remaining vegetative organisms. The spores were centrifuged and resuspended in DMEM and frozen in aliquots at -80°C. The spores were quantified by plating serial dilutions onto taurocholate-fructose-agar plates.

Age- and sex-matched mice were provided water containing kanamycin (0.4 mg/mL), gentamicin (0.035 mg/mL), vancomycin (0.045 mg/mL), colistin (0.057 mg/mL), and metronidazole (0.215 mg/mL) for 5 days. A single dose of clindamycin-2-phosphate (30 mg/kg) was administered 48 hours later by i.p. injection. The mice were orally gavaged 48 hours later with *C. difficile* spores diluted

in 400 μ L DMEM. The mice were monitored daily for survival and symptoms including diarrhea, weight loss, hunched posture, and ruffled fur. To minimize differences in the microbiome, the bedding was randomly mixed among experimental cages for 2 weeks before *C. difficile* inoculation.

Neonatal infections were performed by initiation treatment with water supplemented with the same antibiotics (0.4 mg/mL kanamycin, 0.035 mg/mL gentamicin, 0.045 mg/mL vancomycin, 0.057 mg/mL colistin, and 0.215 mg/mL metronidazole) given to nursing mothers on the day of delivery and for the next 5 days. On day 5 after delivery (and initiation of antibiotic drinking water supplementation), the mothers received a single dose of clindamycin-2-phosphate (30 mg/kg). On day 7 after birth, the neonatal mice were orally gavaged with *C. difficile* (1×10^6 spores in 50 μ L DMEM per pup). On the day of infection, a nursing foster mother (on a WT C57BL/6 background) that had not received antibiotics was placed in the same cage. Infant pups were monitored twice daily from the day of infection until 28 days of life (21 days after infection).

Neutrophil depletion in adult mice. Mice were injected i.p. with 1 mg isotype control (2A3) or anti-Ly6G (1A8) antibodies beginning 1 day before infection, followed by 500 μ g every 48 hours thereafter. Neutrophil depletion was confirmed by flow cytometric analysis of cells from cecal and colonic tissues 2 days after infection.

IL-17A neutralization in adult mice. Mice were injected i.p. with 1 mg isotype control (MOPC-21) or anti-IL-17A (17F3) antibodies beginning 1 day before infection, followed by 500 μ g every 48 hours thereafter.

IL-17A neutralization and $\gamma\delta$ T cell depletion in neonatal mice. Neonatal mice were injected with each depleting/neutralizing or isotype control antibody (100 μ g/50 μ L/pup) beginning 2 days before *C. difficile* spore inoculation and on the day of infection. Survival of infected neonatal mice was monitored for 21 days after infection.

Cell preparation. For isolation of lamina propria cells, whole cecal and colonic tissues were excised and washed in ice-cold PBS to remove digestive contents. Tissues were then cut into 5-mm pieces and incubated in PBS supplemented with 1 mM DTT, 5 mM EDTA, and 3% FCS for 30 minutes at 37°C to remove epithelial cells. The remaining tissues were collected by straining through a 100- μ m filter and homogenized by razor blades, followed by incubation in RPMI supplemented with collagenase type VIII (1 mg/mL; MilliporeSigma) and DNAase I (50 U; MilliporeSigma) for 40 minutes. Cells were strained through a 40- μ m filter into complete RPMI media and collected by centrifugation. For isolation of mLN cells, whole mLNs were excised and crushed using sterile glass slides and then strained through a 40- μ m filter and collected by centrifugation.

Flow cytometry. Cells were kept at 4°C throughout the procedure. Single-cell preparations were incubated with 5% FCS, 2% rat serum, and Fc block for 30 minutes. Without washing, fluorophore-conjugated antibodies were added at the recommended concentration and incubated for an additional 30 minutes in the dark. After 2 washes, dead cells were labeled using a LIVE/DEAD Fixable Violet Dead Cell Stain Kit (Invitrogen, Thermo Fisher Scientific) according to the manufacturer's protocol. Cells were then fixed with 2% paraformaldehyde for 30 minutes before analysis. Data were acquired on a BD LSR II or BD FACSCanto and analyzed with FlowJo software.

Intracellular staining. Cytokine staining was performed using BD Cytofix/Cytoperm (BD Biosciences). Briefly, cells were suspended in media and stimulated with PMA and ionomycin for 5

hours at 37°C. Surface labeling was performed as described above, followed by fixation and permeabilization according to the manufacturer's protocol. Nuclear staining was performed using a FoxP3/Transcription Factor Staining Buffer Set (eBioscience) according to the manufacturer's protocol.

Histology. Cecal and colonic tissues were excised and washed in ice-cold PBS to remove digestive contents and then opened longitudinally with surgical scissors. Tissues were then mounted onto filter paper and fixed in 4% paraformaldehyde for 30 minutes at 4°C. Following incubations in 30% sucrose and 30% sucrose/OCT (Tissue-Tek), tissues were placed into cryomolds and frozen in OCT on a slurry of dry ice and 2-methyl-butane. Tissue blocks were sectioned using a Leica CM1850 Cryostat (Leica Biosystems) and stained with H&E.

Isolation of $\gamma\delta$ T cells. Cells from mLNs were harvested from day-4-infected mice and stimulated with PMA and ionomycin in vitro for 3 hours at 37°C. IL-17A-producing cells were labeled using a Mouse IL-17 Secretion Assay (Miltenyi Biotec) and additionally stained with APC-TCR $\gamma\delta$, PerCP/Cy5.5-TCR β , PerCP/Cy5.5-CD19, and PO-PRO-1 (Invitrogen, Thermo Fisher Scientific) to exclude dead cells. Labeled cells were sorted on a BD FACSAria II (BD Biosciences).

RNA isolation and cDNA synthesis. Following dissection and washing, whole cecum and colonic tissues were cut into 5-mm pieces and immediately homogenized in RNA Bee (Amsbio) using an Omni GLH homogenizer with disposable RNase-Free Probes (Omni International) at 4°C. RNA was extracted according to the manufacturer's protocol. Total RNA was further purified using an RNeasy Mini Kit (QIAGEN). RNA concentration and purity were measured using the Nanodrop 1000 (Thermo Fisher Scientific). cDNA synthesis was performed using a High-Capacity cDNA Reverse Transcription Kit (Thermo Fisher Scientific) according to the manufacturer's instructions. For isolated cells, RNA was extracted using an RNeasy Mini Kit according to the manufacturer's protocol.

qPCR. qPCR of gene expression was performed using TaqMan assays (Applied Biosystems) according to the manufacturer's protocol. TaqMan Gene Expression Master Mix (Applied Biosystems) was used for amplification, and a Mouse GAPDH Endogenous Control (Applied Biosystems) was used as the endogenous control. Data collection was performed using the 7500 Fast System and analyzed by SDS, version 2.4 (Applied Biosystems). The list of TaqMan assays used is included in the supplemental materials.

***tcdB* assay.** Cecal contents were collected and weighed, and total nucleic acids were isolated using a Bacteremia DNA Isolation Kit (BioOstic) according to the manufacturer's instructions. *tcdB* was amplified using Fast SYBR Green Master Mix (Applied Biosystems) with the following primers: 5'-ACGGACAAGCAGTTGAAT-3' and 5'-ATTAATACCTTTGCATGCT-3'.

Tissue explant culture and ELISA. Whole ceca and colons were excised and washed in ice-cold PBS to remove digestive contents, following by rinsing with penicillin and streptomycin. Tissues were weighed, cut into 5-mm pieces, and cultured in complete RPMI at 100 mg/mL for 24 hours. Culture supernatants were collected and analyzed by ELISA for IL-17A/A, IL-17A/F, and IL-17F/F (eBioscience). For mLNs, total cells were stimulated with plate-bound anti-CD3 ϵ and cultured in complete RPMI at 2×10^6 cells/mL for 72 hours. Culture supernatants were collected and analyzed by ELISA as above. For $\gamma\delta$ T cell cultures, mLNs were harvested from day-4-infected mice, and $\gamma\delta$ T cells were isolated using a TCR γ/δ^+ T Cell Isolation Kit (Miltenyi Bio-

tec) according to the manufacturer's protocol. Purified $\gamma\delta$ T cells were cultured in complete RPMI at 2×10^6 cells/mL for 72 hours, under the indicated conditions.

Intestinal permeability assay. Intestinal permeability was measured in *C. difficile*-infected WT and *Il17a*^{-/-} mice by performing oral gavages with FITC-labeled dextran (FD4) and measuring translocation of fluorescence into the plasma. In brief, mice were starved for 6 hours and then orally gavaged with 0.6 mg/g FD4 (MilliporeSigma). Blood was collected via retro-orbital bleeding 3 hours later and allowed to clot for 30 minutes at room temperature. Samples were centrifuged to remove clots, and serum fluorescence was measured on a Synergy HT Microplate Reader (BioTek Instruments).

RNA-Seq and bioinformatics. Library preparation, sequencing, and analysis were performed by the Genome Technology Access Center at the Washington University School of Medicine. Sequencing was performed on a HiSeq 2000 (Illumina) and aligned to the transcriptome with TopHat 1.4.1. Transcript abundance was determined using Cufflinks 2.0.2, and differential gene expression between samples was analyzed by EdgeR and filtered for transcripts passing multiple-testing corrections. Data were deposited in the NCBI's Gene Expression Omnibus (GEO) database (GEO GSE143124).

Statistics. A 2-tailed unpaired *t* test was used unless otherwise noted. *P* values of less than 0.05 were considered statistically significant. Bar graphs and scatter plots show the mean \pm SEM.

Study approval. This prospective cohort study was performed at SLCH (St. Louis, Missouri, USA) with IRB approval from the Washington University School of Medicine. All animal experiments at Washington University and Cincinnati Children's Hospital were IACUC approved and performed at institutions accredited by the Association for Assessment and Accreditation of Laboratory Animal Care (AALAC).

Author contributions

YSC, GP, TYS, SSW, and DBH designed the experiments and analyzed the data. YSC, GP, TYS, and HB performed, analyzed, and interpreted the results of the experiments. IBC analyzed and interpreted the RNA-Seq data. YSC, SSW, and DBH wrote the manuscript.

Acknowledgments

This work was supported by NIH grants U54-AI057160 (Midwest Regional Centers for Excellence for Biodefense and Emerging Infectious Disease Research); P30 DK078392 (Pilot and Feasibility Project of the Digestive Diseases Research Core Center in Cincinnati); 5UL1TR001425-0 (National Center for Advancing Translational Sciences); R21NS064829 (to DBH); R01AI120202 (to SSW); R01AI124657 (to SSW); and DP1AI1131080 (to SSW). SSW is supported by the Howard Hughes Medical Institute (HHMI) Faculty Scholar's program and by a Burroughs Wellcome Fund Investigator in the Pathogenesis Award. The authors thank Celeste Morley for critical review of the manuscript and Ann Kerrigan for assistance with manuscript preparation.

Address correspondence to: David B. Haslam, Division of Infectious Diseases, Cincinnati Children's Hospital Medical Center, 3333 Burnet Avenue, MLC 7017, Ohio 45299, USA. Phone: 513.803.1170; Email: david.haslam@cchmc.org.

1. Dubberke ER, et al. Strategies to prevent *Clostridium difficile* infections in acute care hospitals: 2014 Update. *Infect Control Hosp Epidemiol*. 2014;35(6):628–645.
2. Lessa FC, et al. Burden of *Clostridium difficile* infection in the United States. *N Engl J Med*. 2015;372(9):825–834.
3. Loo VG, et al. A predominantly clonal multi-institutional outbreak of *Clostridium difficile*-associated diarrhea with high morbidity and mortality. *N Engl J Med*. 2005;353(23):2442–2449.
4. Muto CA, et al. A large outbreak of *Clostridium difficile*-associated disease with an unexpected proportion of deaths and colectomies at a teaching hospital following increased fluoroquinolone use. *Infect Control Hosp Epidemiol*. 2005;26(3):273–280.
5. Zilberberg MD, Shorr AF, Kollef MH. Growth and geographic variation in hospitalizations with resistant infections, United States, 2000–2005. *Emerging Infect Dis*. 2008;14(11):1756–1758.
6. Dallal RM, et al. Fulminant *Clostridium difficile*: an underappreciated and increasing cause of death and complications. *Ann Surg*. 2002;235(3):363–372.
7. Pépin J, Valiquette L, Cossette B. Mortality attributable to nosocomial *Clostridium difficile*-associated disease during an epidemic caused by a hypervirulent strain in Quebec. *CMAJ*. 2005;173(9):1037–1042.
8. Chitnis AS, et al. Epidemiology of community-associated *Clostridium difficile* infection, 2009 through 2011. *JAMA Intern Med*. 2013;173(14):1359–1367.
9. Khanna S, et al. The epidemiology of community-acquired *Clostridium difficile* infection: a population-based study. *Am J Gastroenterol*. 2012;107(1):89–95.
10. Jury LA, et al. Outpatient healthcare settings and transmission of *Clostridium difficile*. *PLoS ONE*. 2013;8(7):e70175.
11. Kelly CP, et al. Neutrophil recruitment in *Clostridium difficile* toxin A enteritis in the rabbit. *J Clin Invest*. 1994;93(3):1257–1265.
12. Mylonakis E, Ryan ET, Calderwood SB. *Clostridium difficile*-associated diarrhea: a review. *Arch Intern Med*. 2001;161(4):525–533.
13. Collignon A, Ticchi L, Depitre C, Gaudelus J, Delmée M, Corthier G. Heterogeneity of *Clostridium difficile* isolates from infants. *Eur J Pediatr*. 1993;152(4):319–322.
14. Rousseau C, Poilane I, De Pontual L, Maherault AC, Le Monnier A, Collignon A. *Clostridium difficile* carriage in healthy infants in the community: a potential reservoir for pathogenic strains. *Clin Infect Dis*. 2012;55(9):1209–1215.
15. Rupnik M, Wilcox MH, Gerding DN. *Clostridium difficile* infection: new developments in epidemiology and pathogenesis. *Nat Rev Microbiol*. 2009;7(7):526–536.
16. Abt MC, et al. Innate Immune Defenses mediated by two ILC subsets are critical for protection against acute *Clostridium difficile* infection. *Cell Host Microbe*. 2015;18(1):27–37.
17. Jarchum I, Liu M, Shi C, Equinda M, Pamer EG. Critical role for MyD88-mediated neutrophil recruitment during *Clostridium difficile* colitis. *Infect Immun*. 2012;80(9):2989–2996.
18. Hasegawa M, et al. Nucleotide-binding oligomerization domain 1 mediates recognition of *Clostridium difficile* and induces neutrophil recruitment and protection against the pathogen. *J Immunol*. 2011;186(8):4872–4880.
19. Hasegawa M, Kamada N, Jiao Y, Liu MZ, Núñez G, Inohara N. Protective role of commensals against *Clostridium difficile* infection via an IL-1 β -mediated positive-feedback loop. *J Immunol*. 2012;189(6):3085–3091.
20. Lawley TD, et al. Antibiotic treatment of *Clostridium difficile* carrier mice triggers a supershedder state, spore-mediated transmission, and severe disease in immunocompromised hosts. *Infect Immun*. 2009;77(9):3661–3669.
21. McDermott AJ, Falkowski NR, McDonald RA, Pandit CR, Young VB, Huffnagle GB. Interleukin-23 (IL-23), independent of IL-17 and IL-22, drives neutrophil recruitment and innate inflammation during *Clostridium difficile* colitis in mice. *Immunology*. 2016;147(1):114–124.
22. El Feghaly RE, Stauber JL, Deych E, Gonzalez C, Tarr PI, Haslam DB. Markers of intestinal inflammation, not bacterial burden, correlate with clinical outcomes in *Clostridium difficile* infection. *Clin Infect Dis*. 2013;56(12):1713–1721.
23. El Feghaly RE, Stauber JL, Tarr PI, Haslam DB. Intestinal inflammatory biomarkers and outcome in pediatric *Clostridium difficile* infections. *J Pediatr*. 2013;163(6):1697–1704.e2.
24. Kamada N, Chen GY, Inohara N, Núñez G. Control of pathogens and pathobionts by the gut microbiota. *Nat Immunol*. 2013;14(7):685–690.
25. Ubeda C, Pamer EG. Antibiotics, microbiota, and immune defense. *Trends Immunol*. 2012;33(9):459–466.
26. Tschudin-Sutter S, Widmer AF, Perl TM. *Clostridium difficile*: novel insights on an incessantly challenging disease. *Curr Opin Infect Dis*. 2012;25(4):405–411.
27. Usacheva EA, Jin JP, Peterson LR. Host response to *Clostridium difficile* infection: Diagnostics and detection. *J Glob Antimicrob Resist*. 2016;7:93–101.
28. Jose S, Madan R. Neutrophil-mediated inflammation in the pathogenesis of *Clostridium difficile* infections. *Anaerobe*. 2016;41:85–90.
29. Shibata K, Yamada H, Hara H, Kishihara K, Yoshikai Y. Resident V δ 1⁺ gammadelta T cells control early infiltration of neutrophils after *Escherichia coli* infection via IL-17 production. *J Immunol*. 2007;178(7):4466–4472.
30. Simonian PL, et al. IL-17A-expressing T cells are essential for bacterial clearance in a murine model of hypersensitivity pneumonitis. *J Immunol*. 2009;182(10):6540–6549.
31. Umemura M, et al. IL-17-mediated regulation of innate and acquired immune response against pulmonary *Mycobacterium bovis* bacille Calmette-Guérin infection. *J Immunol*. 2007;178(6):3786–3796.
32. Cho JS, et al. IL-17 is essential for host defense against cutaneous *Staphylococcus aureus* infection in mice. *J Clin Invest*. 2010;120(5):1762–1773.
33. Dejima T, et al. Protective role of naturally occurring interleukin-17A-producing $\gamma\delta$ T cells in the lung at the early stage of systemic candidiasis in mice. *Infect Immun*. 2011;79(11):4503–4510.
34. Curtis MM, Way SS. Interleukin-17 in host defence against bacterial, mycobacterial and fungal pathogens. *Immunology*. 2009;126(2):177–185.
35. Wynn JL, Levy O. Role of innate host defenses in susceptibility to early-onset neonatal sepsis. *Clin Perinatol*. 2010;37(2):307–337.
36. Moens E, Brouwer M, Dimova T, Goldman M, Willems F, Vermijlen D. IL-23R and TCR signaling drives the generation of neonatal V γ 9V δ 2 T cells expressing high levels of cytokine mediators and producing IFN- γ and IL-17. *J Leukoc Biol*. 2011;89(5):743–752.
37. Caccamo N, et al. Differentiation, phenotype, and function of interleukin-17-producing human V γ 9V δ 2 T cells. *Blood*. 2011;118(1):129–138.
38. Chien YH, Zeng X, Prinz I. The natural and the inducible: interleukin (IL)-17-producing $\gamma\delta$ T cells. *Trends Immunol*. 2013;34(4):151–154.
39. Michel ML, Pang DJ, Haque SF, Potocnik AJ, Pennington DJ, Hayday AC. Interleukin 7 (IL-7) selectively promotes mouse and human IL-17-producing $\gamma\delta$ cells. *Proc Natl Acad Sci USA*. 2012;109(43):17549–17554.
40. Gibbons DL, et al. Neonates harbour highly active gammadelta T cells with selective impairments in preterm infants. *Eur J Immunol*. 2009;39(7):1794–1806.
41. McElroy SJ, Weitkamp JH. Innate immunity in the small intestine of the preterm infant. *Neoreviews*. 2011;12(9):e517–e526.
42. Duan J, Chung H, Troy E, Kasper DL. Microbial colonization drives expansion of IL-1 receptor 1-expressing and IL-17-producing gamma/delta T cells. *Cell Host Microbe*. 2010;7(2):140–150.
43. Hirota SA, et al. Intrarectal instillation of *Clostridium difficile* toxin A triggers colonic inflammation and tissue damage: development of a novel and efficient mouse model of *Clostridium difficile* toxin exposure. *Infect Immun*. 2012;80(12):4474–4484.
44. Reeves AE, Koenigsnecht MJ, Bergin IL, Young VB. Suppression of *Clostridium difficile* in the gastrointestinal tracts of germfree mice inoculated with a murine isolate from the family Lachnospiraceae. *Infect Immun*. 2012;80(11):3786–3794.
45. Chen X, et al. A mouse model of *Clostridium difficile*-associated disease. *Gastroenterology*. 2008;135(6):1984–1992.
46. Reeves AE, Theriot CM, Bergin IL, Huffnagle GB, Schloss PD, Young VB. The interplay between microbiome dynamics and pathogen dynamics in a murine model of *Clostridium difficile* infection. *Gut Microbes*. 2011;2(3):145–158.
47. Buffie CG, et al. Profound alterations of intestinal microbiota following a single dose of clindamycin results in sustained susceptibility to *Clostridium difficile*-induced colitis. *Infect Immun*. 2012;80(1):62–73.
48. Pawlowski SW, et al. Murine model of *Clostridium difficile* infection with aged gnotobiotic C57BL/6 mice and a BI/NAP1 strain. *J Infect Dis*. 2010;202(11):1708–1712.
49. MacDougall LK, et al. Comparison of qPCR versus culture for the detection and quantification of *Clostridium difficile* environmental contamination. *PLoS ONE*. 2018;13(8):e0201569.
50. Etienne-Mesmin L, et al. Genome sequence of a toxin-positive *Clostridium difficile* strain isolated from murine feces. *Genome Announc*. 2017;5(14):e00088–17.
51. Etienne-Mesmin L, Chassaing B, Adekunle O, Mattei LM, Bushman FD, Gewirtz AT. Toxin-positive *Clostridium difficile* latently infect mouse

- colonies and protect against highly pathogenic *C. difficile*. *Gut*. 2018;67(5):860–871.
52. McGeachy MJ, Cua DJ, Gaffen SL. The IL-17 family of cytokines in health and disease. *Immunity*. 2019;50(4):892–906.
 53. Amatya N, Garg AV, Gaffen SL. IL-17 signaling: the yin and the yang. *Trends Immunol*. 2017;38(5):310–322.
 54. Itohara S, et al. T cell receptor delta gene mutant mice: independent generation of alpha beta T cells and programmed rearrangements of gamma delta TCR genes. *Cell*. 1993;72(3):337–348.
 55. Wilharm A, et al. Mutual interplay between IL-17-producing $\gamma\delta$ T cells and microbiota orchestrates oral mucosal homeostasis. *Proc Natl Acad Sci USA*. 2019;116(7):2652–2661.
 56. Dejima T, et al. Protective role of naturally occurring interleukin-17A-producing $\gamma\delta$ T cells in the lung at the early stage of systemic candidiasis in mice. *Infect Immun*. 2011;79(11):4503–4510.
 57. Akitsu A, Iwakura Y. Interleukin-17-producing $\gamma\delta$ T ($\gamma\delta$ 17) cells in inflammatory diseases. *Immunology*. 2018;155(4):418–426.
 58. Bonneville M, O'Brien RL, Born WK. Gammadelta T cell effector functions: a blend of innate programming and acquired plasticity. *Nat Rev Immunol*. 2010;10(7):467–478.
 59. Thedrez A, et al. Self/non-self discrimination by human gammadelta T cells: simple solutions for a complex issue? *Immunol Rev*. 2007;215:123–135.
 60. Zeng X, et al. $\gamma\delta$ T cells recognize a microbial encoded B cell antigen to initiate a rapid antigen-specific interleukin-17 response. *Immunity*. 2012;37(3):524–534.
 61. Sumaria N, Martin S, Pennington DJ. Developmental origins of murine $\gamma\delta$ T-cell subsets. *Immunology*. 2019;156(4):299–304.
 62. McKenzie DR, Comerford I, Silva-Santos B, McColl SR. The emerging complexity of $\gamma\delta$ T17 cells. *Front Immunol*. 2018;9:796.
 63. Lefranc MP, Lefranc G. IMGT[®] and 30 years of immunoinformatics insight in antibody V and C domain structure and function. *Antibodies (Basel)*. 2019;8(2):E29.
 64. Narayan K, et al. Intrathymic programming of effector fates in three molecularly distinct $\gamma\delta$ T cell subtypes. *Nat Immunol*. 2012;13(5):511–518.
 65. Malhotra N, et al. A network of high-mobility group box transcription factors programs innate interleukin-17 production. *Immunity*. 2013;38(4):681–693.
 66. Chien YH, Meyer C, Bonneville M. $\gamma\delta$ T cells: first line of defense and beyond. *Annu Rev Immunol*. 2014;32:121–155.
 67. Papotto PH, Reinhardt A, Prinz I, Silva-Santos B. Innately versatile: $\gamma\delta$ 17 T cells in inflammatory and autoimmune diseases. *J Autoimmun*. 2018;87:26–37.
 68. Sumaria N, Grandjean CL, Silva-Santos B, Pennington DJ. Strong TCR $\gamma\delta$ signaling prohibits thymic development of IL-17A-secreting $\gamma\delta$ T Cells. *Cell Rep*. 2017;19(12):2469–2476.
 69. Marchitto MC, et al. Clonal V γ 6⁺V δ 4⁺ T cells promote IL-17-mediated immunity against *Staphylococcus aureus* skin infection. *Proc Natl Acad Sci USA*. 2019;116(22):10917–10926.
 70. Lockhart E, Green AM, Flynn JL. IL-17 production is dominated by gammadelta T cells rather than CD4 T cells during *Mycobacterium tuberculosis* infection. *J Immunol*. 2006;177(7):4662–4669.
 71. Sutton CE, Lalor SJ, Sweeney CM, Brereton CF, Lavelle EC, Mills KH. Interleukin-1 and IL-23 induce innate IL-17 production from gammadelta T cells, amplifying Th17 responses and autoimmunity. *Immunity*. 2009;31(2):331–341.
 72. Cai Y, et al. Pivotal role of dermal IL-17-producing $\gamma\delta$ T cells in skin inflammation. *Immunity*. 2011;35(4):596–610.
 73. Lu Y, Cao X, Zhang X, Kovalovsky D. PLZF controls the development of fetal-derived IL-17⁺V γ 6⁺ $\gamma\delta$ T cells. *J Immunol*. 2015;195(9):4273–4281.
 74. Haas JD, et al. Development of interleukin-17-producing $\gamma\delta$ T cells is restricted to a functional embryonic wave. *Immunity*. 2012;37(1):48–59.
 75. Chien YH, Zeng X, Prinz I. The natural and the inducible: interleukin (IL)-17-producing $\gamma\delta$ T cells. *Trends Immunol*. 2013;34(4):151–154.
 76. Spidale NA, et al. Interleukin-17-producing $\gamma\delta$ T cells originate from SOX13⁺ progenitors that are independent of $\gamma\delta$ TCR signaling. *Immunity*. 2018;49(5):857–872.e5.
 77. Ribot JC, et al. CD27 is a thymic determinant of the balance between interferon-gamma- and interleukin 17-producing gammadelta T cell subsets. *Nat Immunol*. 2009;10(4):427–436.
 78. Corpuz TM, et al. IL-2 shapes the survival and plasticity of IL-17-producing $\gamma\delta$ T cells. *J Immunol*. 2017;199(7):2366–2376.
 79. Powolny-Budnicka I, Riemann M, Tänzler S, Schmid RM, Hehlhans T, Weih F. RelA and RelB transcription factors in distinct thymocyte populations control lymphotoxin-dependent interleukin-17 production in $\gamma\delta$ T cells. *Immunity*. 2011;34(3):364–374.
 80. Selber-Hnatiw S, et al. Human Gut Microbiota: Toward an Ecology of Disease. *Front Microbiol*. 2017;8:1265.
 81. Laird RM, Wolf BJ, Princiotta MF, Hayes SM. $\gamma\delta$ T cells acquire effector fates in the thymus and differentiate into cytokine-producing effectors in a *Listeria* model of infection independently of CD28 costimulation. *PLoS ONE*. 2013;8(5):e63178.
 82. Zuberbuehler MK, et al. The transcription factor c-Maf is essential for the commitment of IL-17-producing $\gamma\delta$ T cells. *Nat Immunol*. 2019;20(1):73–85.
 83. Koenecke C, Chennupati V, Schmitz S, Malissen B, Förster R, Prinz I. In vivo application of mAb directed against the gammadelta TCR does not deplete but generates “invisible” gammadelta T cells. *Eur J Immunol*. 2009;39(2):372–379.
 84. Cypowij S, Picard C, Maródi L, Casanova JL, Puel A. Immunity to infection in IL-17-deficient mice and humans. *Eur J Immunol*. 2012;42(9):2246–2254.
 85. Simonian PL, et al. Regulatory role of gammadelta T cells in the recruitment of CD4⁺ and CD8⁺ T cells to lung and subsequent pulmonary fibrosis. *J Immunol*. 2006;177(7):4436–4443.
 86. Hamada S, et al. Importance of murine Vdelta1gammadelta T cells expressing interferon-gamma and interleukin-17A in innate protection against *Listeria* monocytogenes infection. *Immunology*. 2008;125(2):170–177.
 87. McDermott AJ, Frank CR, Falkowski NR, McDonald RA, Young VB, Huffnagle GB. Role of GM-CSF in the inflammatory cytokine network that regulates neutrophil influx into the colonic mucosa during *Clostridium difficile* infection in mice. *Gut Microbes*. 2014;5(4):476–484.
 88. Nakagawa T, et al. Endogenous IL-17 as a factor determining the severity of *Clostridium difficile* infection in mice. *J Med Microbiol*. 2016;65(8):821–827.
 89. Ng J, et al. *Clostridium difficile* toxin-induced inflammation and intestinal injury are mediated by the inflammasome. *Gastroenterology*. 2010;139(2):542–552, 552.e1.
 90. Moens E, Brouwer M, Dimova T, Goldman M, Willems F, Vermijlen D. IL-23R and TCR signaling drives the generation of neonatal Vgamma9Vdelta2 T cells expressing high levels of cytotoxic mediators and producing IFN-gamma and IL-17. *J Leukoc Biol*. 2011;89(5):743–752.
 91. Hasegawa M, et al. Interleukin-22 regulates the complement system to promote resistance against pathobionts after pathogen-induced intestinal damage. *Immunity*. 2014;41(4):620–632.
 92. Sawa S, et al. ROR γ t⁺ innate lymphoid cells regulate intestinal homeostasis by integrating negative signals from the symbiotic microbiota. *Nat Immunol*. 2011;12(4):320–326.
 93. Korn LL, et al. Conventional CD4⁺ T cells regulate IL-22-producing intestinal innate lymphoid cells. *Mucosal Immunol*. 2014;7(5):1045–1057.
 94. Caccamo N, et al. Differentiation, phenotype, and function of interleukin-17-producing human V γ 9V δ 2 T cells. *Blood*. 2011;118(1):129–138.
 95. Martin B, Hirota K, Cua DJ, Stockinger B, Veldhoen M. Interleukin-17-producing gammadelta T cells selectively expand in response to pathogen products and environmental signals. *Immunity*. 2009;31(2):321–330.
 96. Jouan Y, Patin EC, Hassane M, Si-Tahar M, Baranek T, Paget C. Thymic Program Directing the Functional Development of gammadelta T17 Cells. *Front Immunol*. 2018;9:981.
 97. Sutton CE, Lalor SJ, Sweeney CM, Brereton CF, Lavelle EC, Mills KH. Interleukin-1 and IL-23 induce innate IL-17 production from gammadelta T cells, amplifying Th17 responses and autoimmunity. *Immunity*. 2009;31(2):331–341.
 98. Lalor SJ, Dungan LS, Sutton CE, Basdeo SA, Fletcher JM, Mills KH. Caspase-1-processed cytokines IL-1beta and IL-18 promote IL-17 production by gammadelta and CD4 T cells that mediate autoimmunity. *J Immunol*. 2011;186(10):5738–5748.
 99. Jensen KD, et al. Thymic selection determines gammadelta T cell effector fate: antigen-naive cells make interleukin-17 and antigen-experienced cells make interferon gamma. *Immunity*. 2008;29(1):90–100.
 100. Dillen CA, et al. Clonally expanded $\gamma\delta$ T cells protect against *Staphylococcus aureus* skin reinfection. *J Clin Invest*. 2018;128(3):1026–1042.
 101. Sheridan BS, et al. Gammadelta T cells exhibit multifunctional and protective memory in intestinal tissues. *Immunity*. 2013;39(1):184–195.
 102. Haas JD, et al. Development of interleukin-17-producing $\gamma\delta$ T cells is restricted to a functional embryonic wave. *Immunity*. 2012;37(1):48–59.
 103. Gibbons DL, et al. Suppression of airway inflammation by a natural acute infection of the intestinal epithelium. *Mucosal Immunol*. 2009;2(2):144–155.
 104. Lyras D, et al. Toxin B is essential for virulence of *Clostridium difficile*. *Nature*. 2009;458(7242):1176–1179.